

RESEARCH

Open Access



# Enhanced radiation characteristics of regular dodecagon split ring resonator (D-SRR)-based microstrip patch antenna employing dielectric superstrate for THz applications

Kaddour Benkhallouk<sup>1</sup>, Amina Bendaoudi<sup>1\*</sup> , Mohammed Berka<sup>2</sup> and Zoubir Mahdjoub<sup>1</sup>

\*Correspondence:  
aminabendaoudi@yahoo.fr

<sup>1</sup> Electronic Department, Djillali Liabes University of Sidi Bel Abbés, 22000 Sidi Bel Abbés, Algeria

<sup>2</sup> Electronic Department, Mustapha Stambouli University of Mascara, Mascara, Algeria

## Abstract

In a world where communication requires ever faster data transmission capable of transmitting high speeds. In order to reach and transmit this high speed, it is necessary to increase the frequency that carries the information. For this, scientists are interested in the terahertz (THz) range which, thanks to its high frequencies between 0.1 THz and 30 THz, offers the possibility of increasing the data rate. This letter presents the inclusion of Dodecagon Split Ring Resonator (D-SRR) in rectangular microstrip patch antenna and its effect in the performance of the proposed antenna. The metamaterial design employs two types of SRRs resonators shapes such as the Dodecagon Broadside Coupled Split Ring Resonator (DBC-SRR) and Dodecagon Split Ring Resonator (D-SRR). The model applied uses a local field approach and allowed to obtain the dispersion characteristics of discrete negative magnetic permeability. The proposed antenna substrate uses Arlon AD1000 material, which helps to attain high gain and good directivity at THz frequency. The antenna performance is investigated with and without superstrate. The operating frequencies of the proposed antenna vary in the range of 0.66 - 0.69 THz and shows maximum gain of 10.4 dB and maximum directivity of 9.84 dB. HFSS software tool helps to simulate the parametric analysis of the proposed antenna design. This novel structure may find applications in terahertz imaging, remote systems and may find manifold possibilities in the medical field.

**Keyword:** Microstrip patch antennas, DBC-SRR resonator, D-SRR resonator, Metamaterial, Terahertz band

## Introduction

The next generation requires advance applications in the field of wireless communications, which depends on the development of tiny, faster, more efficient, and cost-effective ultra-broadband antenna [1], and the communication systems focus on THz region for increased carrier frequency, higher data rates, and high channel capacity [2]. However, THz waves, which are located between millimeter waves and infrared light waves in the electromagnetic spectrum, had rarely been utilized [3], in communications, radar, imaging, sensors, astronomy, space-science, and ultra-fast chemistry [4, 5]. At the terahertz frequency, the

implementation of the antenna is the matter of research in goal to enhance the electrical performance of the microstrip antenna in terms of reflection coefficient, gain, and directivity.

The microstrip antenna printed on dielectric substrates have been successful in applications requiring low profiles and compactness [6]. The size of an antenna reduces to submillimeter at Terahertz frequencies [6, 7]. Due to advancement in photonics and semiconductor devices, which are operating at terahertz frequency, the realization of these submillimeter systems is possible [8]. Metamaterials are the most critical part determining whether a system will be practical and capable to having an active role in modern wireless communications. The metamaterials studied by the Russian physicist Victor Veselago are pseudo-homogeneous artificial or composite structures possessing electromagnetic properties not available in nature [9]. Later, Smith implements first left-handed materials consist of periodic split-ring resonators (SRRs) and long strips [10, 11]. SRRs are well known in metamaterials since they can provide negative permeability that can create a stopband response at the resonant frequency [12, 13] and also produce new bands of operation [14–17]. Since the rings are broadside-coupled in the SRR resonator, it will be called broadside-coupled SRR (BC-SRR) [18]. The possibilities of changing the resonance frequency by varying the spacing between the two rings of the BC-SRR in response to the amplitude of vibration in a controllable and sensitive way makes it an ideal candidate among different SRR structures for the proposed sensor [19].

More recently, several researchers have been working on the implementation of techniques and systems in order to be able to use it in higher-speed communication. Several articles covering the different aspects of this subject (communication sources and detectors, modulation systems, wireless communication measurements). Microstrip patch antennas are increasingly popular in sensing applications. For pH sensor application, M-Tariqul et al. [20] proposed a ultrawideband antenna based on Hexagonal Split-Ring Resonator with small electrical size can reach a high gain and bandwidth. The authors [21] designed a microwave dual-band metamaterial perfect absorber based on one square patch with 45° diagonal slot structure, which achieved two absorption band and able to change with different polarization angles. Besides, Yadgar et al. [22] proposed a sandwich metamaterial in a frequency band of left-hand characteristics in a range of 8–18 GHz and the resonant absorption is dominated by the induced magnetic dipole.

The objective of this paper is to enhance and improve the coefficient of reflection, bandwidth, and gain of a conventional microstrip antenna using a different approach while applying the Dodecagon Split Ring Resonators (D-SRR) or Dodecagon Broadside Coupled Split Ring Resonator (DBC-SRR). The resonators patterned structures are directly lay on the upper of the patch or on the dielectric substrate; therefore, the microstrip antenna can have an excellent performances. Then, we investigate the effect of superstrate on directivity and radiation pattern. The designed antenna loaded with metamaterial resonators is numerically simulated and investigated. The details of the proposed antennas design and the results are presented in the following sections.

## Methods

The main aim of this paper is to design a novel microstrip antenna using a different approach of metamaterials without degrading the other performance parameters of antenna.

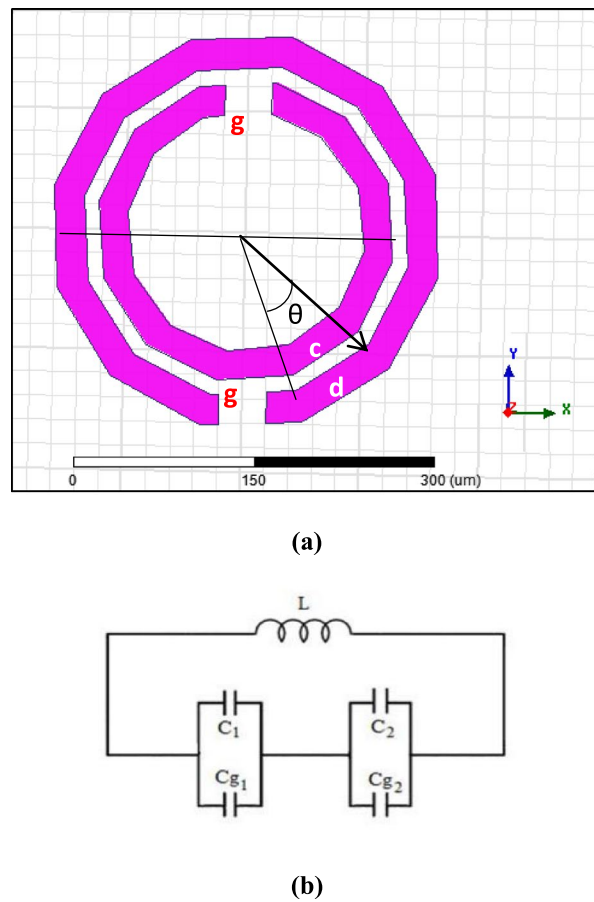


**Fig. 1** Structure of dodecagon SRR. **a** Representation in rings. **b** Equivalent electrical circuit [25]

### Theoretical background of the proposed SRR cell

#### Structure design of the dodecagon SRR

A split-ring resonator (SRR) is an artificially created structure allow provoking magnetic susceptibility in various types of metamaterials up to 200 THz. In addition, the magnetic resonance is induced by the gap between inner and outer rings. The SRR varies in its shape and structure such as square SRR and circular SRR [23–25]. The rarer structures include multiple SRR, spiral SRR, triangular SRR, and elliptical SRR [26–30]. In this work, we propose a new model of SRR as a regular dodecagon with twelve angles and therefore twelve sides. The structure of dodecagon split-ring resonator (DSRR) is illustrated in Fig. 1.

The resonant frequency ( $f_0$ ) of the regular dodecagon SRR is given by [25–31]:

$$f_0 = \frac{1}{(2\pi\sqrt{2 \cdot a_{eq} \cdot L_{Net} \cdot C_{Net}})} \quad (1)$$

where  $a_{eq}$  is the effective radius of regular dodecagon SRR and its expression is [25–31]:

$$a_{eq} = 2a \cdot \sin \left\{ \frac{\pi}{N} \right\} - \frac{g}{N} \quad (2)$$

So, in our case  $N=12$ .

$L_{Net}$  is the equivalent inductance and its expression is [25–31]:

$$L_{Net} = 0.00508 * \left( 2.303 \log_{10} \frac{4l}{c} - 2.636 \right) \quad (3)$$

where  $c$  is the width of the strip,  $l$  is the perimeter of the regular dodecagon SRR, and the expression of  $l$  is shown in the following equation [25–31]:

$$l = 2 \cdot a \cdot N \cdot \sin \frac{\pi}{N} \quad (4)$$

$C_{Nett}$  is the equivalent capacitance of the structure and the expression is [25–31]:

$$C_{Net} = \left\{ \frac{(N \cdot \sin \frac{\pi}{N} + \beta)^2 - (\frac{\Delta}{a})^2}{2(N \cdot \sin \left\{ \frac{\pi}{N} \right\} + \beta)} \right\} \quad (5)$$

where  $\beta = C_g/a$ .  $C_{pul}$  and  $C_{pul}$  is the capacitance per unit length of the regular dodecagon SRR and [25]:

$$\Delta = a \cdot \sin \left\{ \frac{\pi}{N} \right\} \cdot (2m + 1) - a \cdot \cos \left\{ \frac{\pi}{N} \right\} \cdot \tan \left\{ \frac{\pi}{N} - \varphi \right\} \quad (6)$$

Now, the capacitance of the upper half-ring ( $C_u$ ) and lower half-ring ( $C_l$ ) can be easily computed from  $\Delta$  and  $C_{pul}$  as [25–31]:

$$C_u = \left[ N \cdot a \cdot \sin \left\{ \frac{\pi}{N} \right\} - \Delta \right] \cdot C_{pul} \quad (7)$$

And:

$$C_l = \left[ N \cdot a \cdot \sin \left\{ \frac{\pi}{N} \right\} + \Delta \right] \cdot C_{pul} \quad (8)$$

$C_g$  is the capacitance due to the split gaps in the rings and can be estimated using the equation [25–31]:

$$C_g = \frac{\epsilon_0 \cdot \epsilon_r \cdot C \cdot h}{g} \quad (9)$$

where  $\epsilon_0$  is the permittivity of free space ( $\epsilon_0 = 8.8541 \times 10^{-12}$  F/mt) and  $\epsilon_r$  is the relative permittivity which is different for materials [25].

### Structure design of dodecagon broadside coupled SRR

In the broadside-coupled split ring resonator (BC-SRR) structure, the rings are printed on both sides of the dielectric substrate with slit locations  $180^\circ$  apart. A dodecagon broadside-coupled split-ring resonator (DBC-SRR) is depicted in Fig. 2. It consists of two face-to-face coupled rings and they etched in parallel planes with splits on opposite sides.

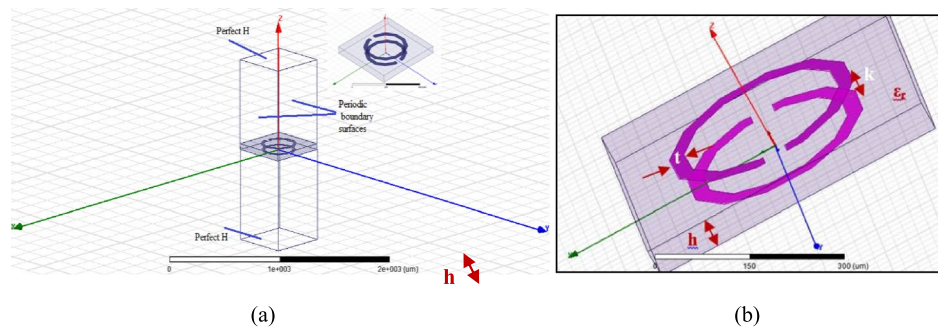


**Fig. 2** Structure of dodecagon broadside coupled SRR. **a** Simulation model of proposed a structure between two waveguide ports in HFSS and **b** back view of DC-SRR

**Table 1** Dimensions of DBC-SRR structure

Parameters	Size (μm)
$K$	0.09
$t$	0.02
$h$	0.09
$\epsilon_r$	4.4

The dimensions of DBC-SRR structure are summarized in Table 1. The resonator is etched on substrate namely FR4 epoxy dielectric material with relative permittivity ( $\epsilon_r$ ) of 4.4 and with thickness  $h=0.09 \mu\text{m}$ . The operation of the dodecagon broadside-coupled resonator near the 12 THz band.

The result of reflection and transmission coefficients as a function of the frequency of an SRR cell unit are displayed in Fig. 3

From Fig. 3, we observe on the curve of  $S_{11}$  a resonant frequency at 11.44 THz with a transmission of the order of  $-63 \text{ dB}$ . On the  $S_{21}$  curve, we observe a high bandwidth transmission at 12.43 GHz.

### Pattern antenna project

The pattern antenna project was developed through the parameters of the rectangular microstrip antenna, which has a microstrip line power and the patch is made by copper, as in Fig. 4, in which is based on the transmission line method theory, that means, operation frequency of 0.65 THz. The resonance frequency is obtained in [32]:

$$f_r = \frac{C}{2.L \sqrt{\epsilon_r}} \quad (10)$$

where  $C$  is the speed of light in free space,  $L$  is length, and  $\epsilon_r=10.2$  (Arlon AD1000) is the dielectric constant of the substrate.

The dimensions of proposed microstrip antenna are summarized in Table 2.

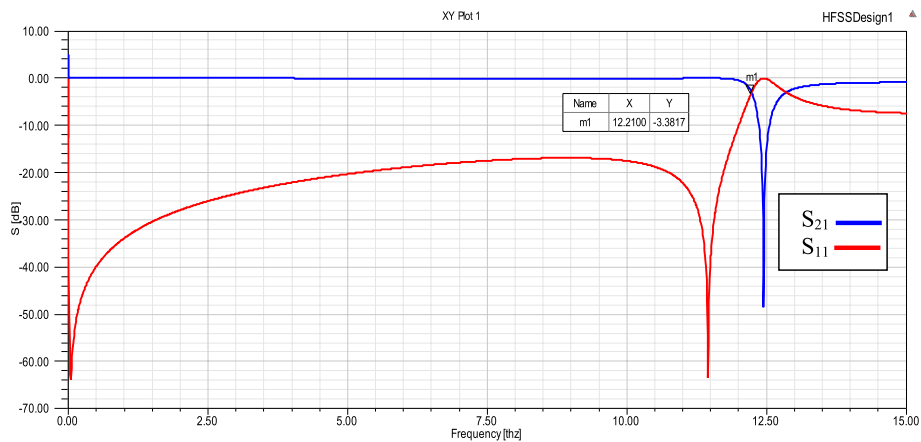


Fig. 3 Simulated reflection and transmission coefficient

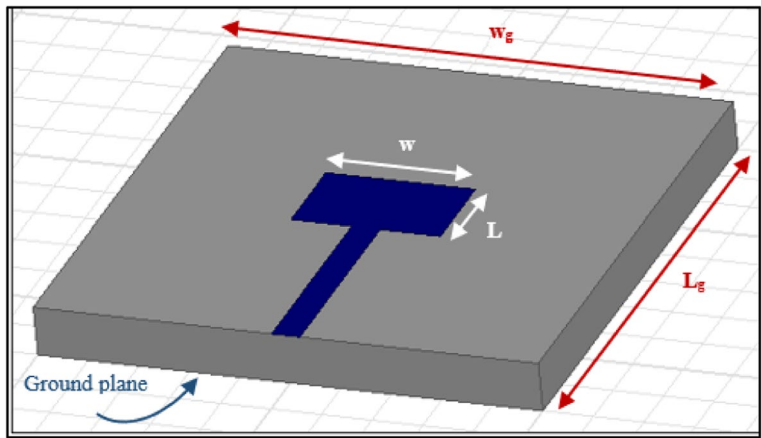


Fig. 4 Microstrip antenna dimensions

Table 2 Dimensions of microstrip antenna

Parameters	Size (μm)
Length of the radiating patch (L)	89
Width of the radiating patch (W)	148
Length of the 50 Ω line (L)	250
Width of the 50Ω line (W)	28
Length of the ground plane (L <sub>g</sub> )	500
Width of the ground plane (W <sub>g</sub> )	500

Simulation results and discussion

Dodecagon SRR behavior

On the upper surface of the glass substrate ( $\epsilon_r= 5.5$ ), the regular dodecagon metamaterial resonator SRR (D-SRR) is printed for a thickness equal to 0.003  $\mu\text{m}$ . The Fig. 5 represent the 3-D Modeler of the HFSS simulator:

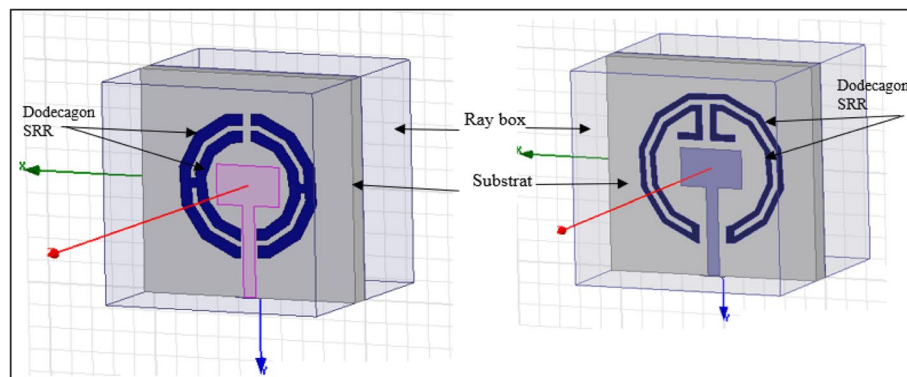


**Fig. 5** Proposed shapes of dodecagon resonator in HFSS

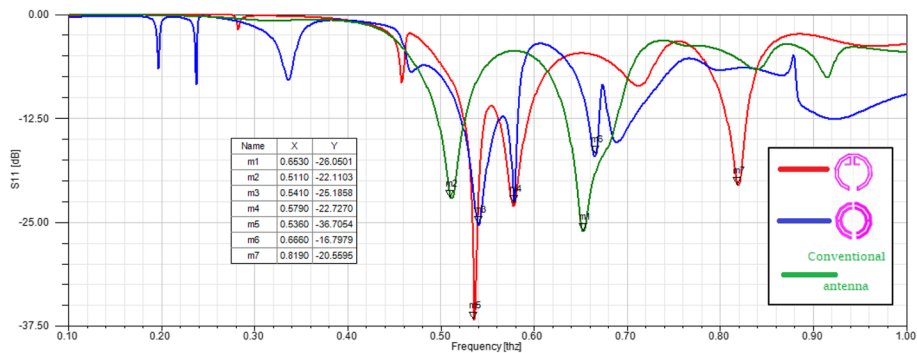


**Fig. 6** Simulated reflection coefficient of microstrip patch antenna loaded with D-SRR

Figure 6 shows the simulated reflection coefficient between 0.1 and 1 THz for two different shapes of D-SRR

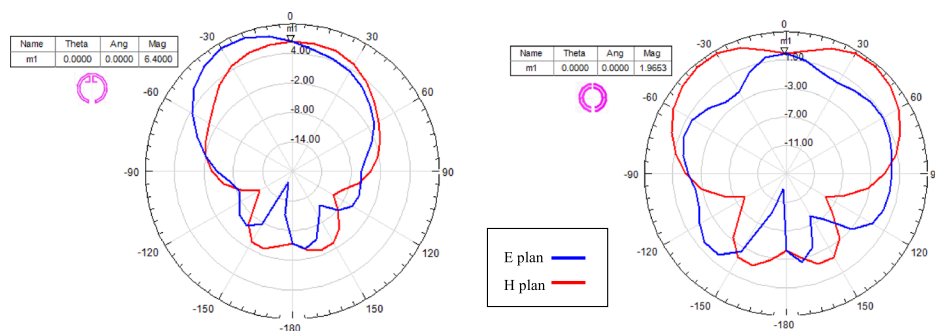
From the results in Fig. 6, a significant difference was observed. The two proposed shapes of D-SRR have a multi-band characteristic in the spectrum, and the resonant frequencies are located at 0.54, 0.57, 0.53, 0.66, and 0.81 THz. The results proves the multi-band characteristics of the proposed structure.

Figure 7 illustrate the radiation patterns in H plane and E plane cuts for the two proposed antennas.

#### **Dodecagon BC-SRR-loaded microstrip patch antenna**

**DBC-SRR loaded vertically microstrip patch antenna** Figure 8 display the arrangement of the proposed design for the microstrip antenna and DBC-SRR for positive and beam-deflection with 1 layer, 2 layers, and 3 layers, respectively. In this context, we propose to deviate the beam toward the positive angles so that the arrangement of DBC-SRR must be placed on the right side of the microstrip patch antenna. We notice that the deflection angle increase proportionally with number of layers. Each linear array of DB-CSRR has a spacing of 5  $\mu\text{m}$ , and between linear arrays, the spacing is 5  $\mu\text{m}$ .





**Fig. 7** Simulated radiation patterns of microstrip patch antenna loaded with D-SRR

The dielectric substrate used is a low loss PVC foam sheet of thickness  $10\text{ }\mu\text{m}$  having relative permittivity 1.2 and dielectric loss tangent 0.001. The surface area of the substrate is  $96\text{ }\mu\text{m} \times 96\text{ }\mu\text{m}$ . The two rings are separately etched from thin sheets of copper with a thickness of  $10\text{ }\mu\text{m}$ . The outer and inner radius of the rings are designed as 36 mm and 26 mm, respectively, and the slit width is  $40\text{ }\mu\text{m}$ .

Figure 9 represents the radiation patterns in H plane and E plane cuts for the microstrip antenna with DBC-SRR structure.

Figures 9a–d presents the radiation pattern for the microstrip antenna with DBC-SRR structure. In the first simulation with one array of DBC-SRR, the radiation beam is tilted by an angle of  $+30^\circ$  in the E-plane at 0.65 THz and the gain is equal to  $-3.7\text{ dB}$ . When we add another layer, the radiation beam is tilted by an angle at  $+30^\circ$  and the gain is increase to  $-4.5\text{ dB}$ . The radiation beam is tilted when the antenna is loaded with Three array of DBC-SRR and the gain become  $-5.5\text{ dB}$ . The simulated result confirms that the main beam is deflected by  $+30^\circ$ . To carry out a negative tilting angle, the arrangement of the DBC-SRR structure is reversed on the left side of the microstrip patch antenna. The

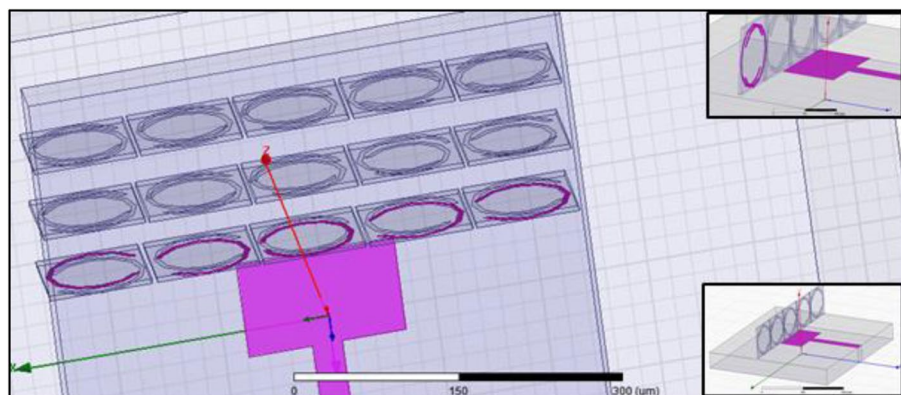


**Fig. 8** DBC-SRR loaded vertically microstrip patch antenna



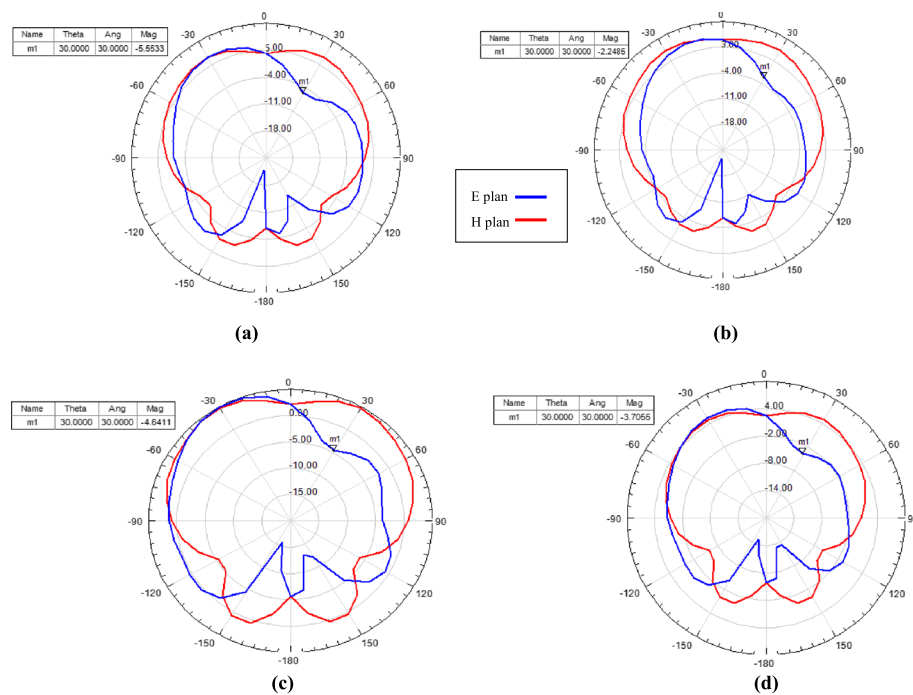


**Fig. 9** The radiation pattern for the microstrip antenna with DBC-SRR structure at 0.65 THz. **a** Conventional antenna, **b** antenna with one array of DBC-SRR, **c** two arrays, and **d** three arrays

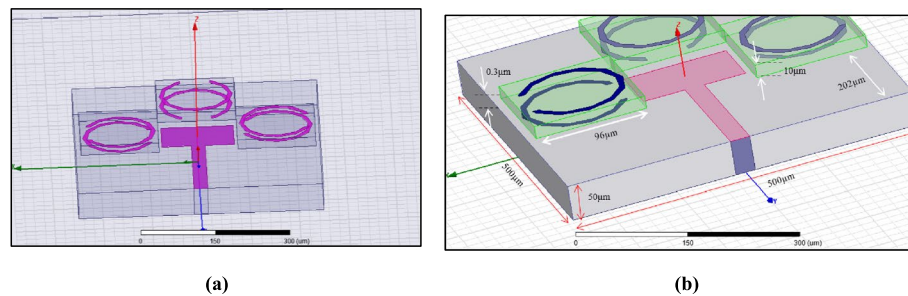


**Fig. 10** DBC-SRR loaded horizontally microstrip patch antenna. **a** Model in HFSS. **b** Dimensions of proposed structure

including of DBC-SRR array affects the shape of the radiation pattern in E-plane; however, the proposed antenna still radiates with no tilting for both directions as illustrated in Fig. 11.

**DBC-SRR loaded horizontally microstrip patch antenna** The layout of the DBC-SRR loaded on the microstrip patch antenna is given in Fig. 10. In this part, three DSRR unit cell will be placed horizontally in a parallel way with the substrate of the proposed antenna. The three D-SRR unit cell is fixed on the opposite sides of a low loss PVC foam substrate of thickness 10  $\mu\text{m}$ , and the combination is fixed very near (0.3  $\mu\text{m}$ ) and around to the microstrip patch antenna.

The simulated  $S_{11}$  characteristics of the DBC-SRR-loaded microstrip antenna structure versus frequency using HFSS simulation software are depicted in Fig. 11.

We notice the first resonant mode between the antenna and the DBC-SRR that there was an increase in the parameter values  $S_{11}$  of about  $-26$  dB, besides the frequency displacement from the loaded antenna by metamaterials, which is due to the change in electromagnetic parameters of permittivity and permeability of the material applied on the substrate. However, for the second resonant mode, the microstrip patch antenna with DBC-SRR displayed a decrease in the parameter values  $S_{11}$  adding to the little increase in width band for the second resonant mode.

In Fig. 12, a significance difference was apparent in the radiation patterns of the microstrip patch antenna with DBC-SRR. The radiation of the antenna and the radiated energy own the same direction and is concentrated in the main lobe.

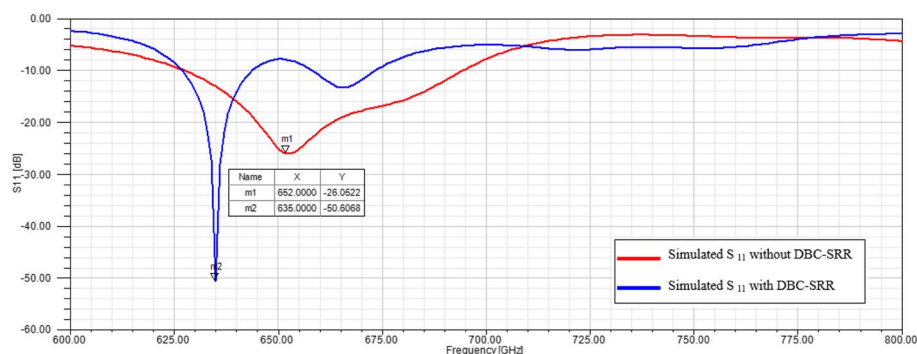
The simulation demonstrates an asymmetrical radiation pattern about the broadside direction across antenna bandwidth with gain of 1.91 and 3dB beam width of  $50^\circ$  in the H plane and  $40^\circ$  in the E plane, whereas the radiation pattern of conventional microstrip patch antenna has a gain equal to 5.04dB and 3dB beam width of  $140^\circ$  in the H plane and  $40^\circ$  in the E plane.

*The behavior of the periodic arrays of the D-SRR* Based on the idea of [33] about the behavior of toothed SRR, the patch has several slots dodecagon-shaped and arranged on its surface and inside each shape is printed a D-SRR cell unit. Figure 13 represents rectangular patch antenna with an array of D-SRR.

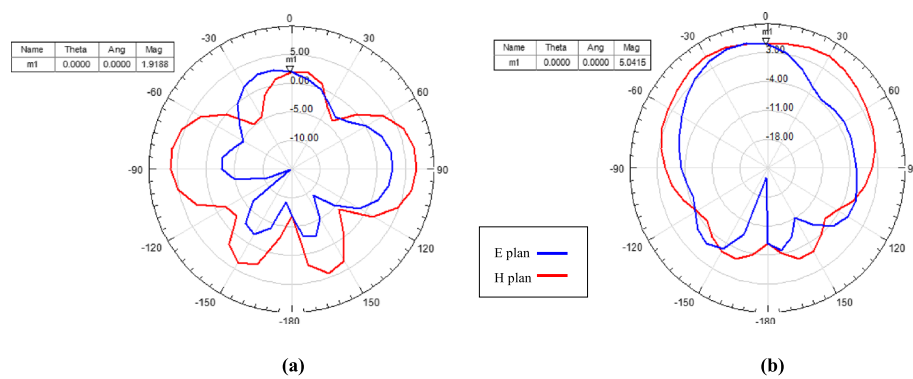
Figure 14 represents the simulated  $S_{11}$  for the microstrip patch antenna in terms of number of the SRR resonators put on the patch that form the array.

Table 3 illustrates the comparative study and analysis of simulated antenna in terms of resonance frequency, coefficient  $S_{11}$ , and the with band.

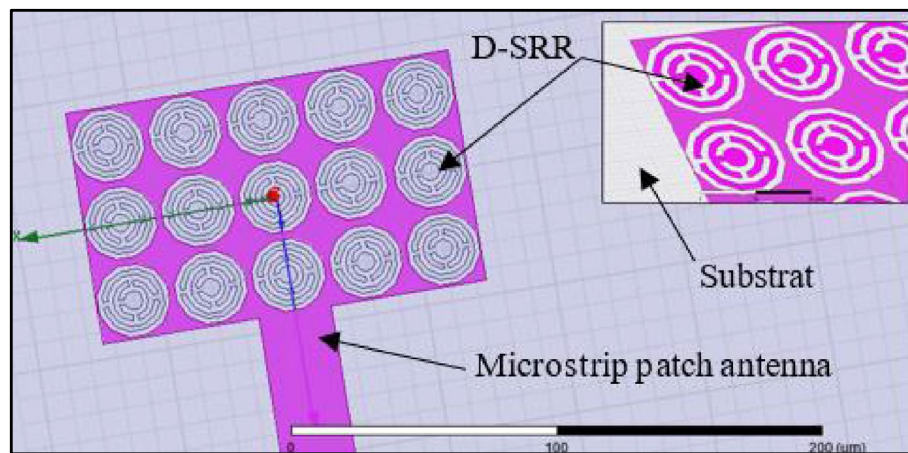
According to the Table 3 results, the proposed patch keeps dual band, as well the principal resonant mode of resonance. For these resonant modes, we notice that the frequency



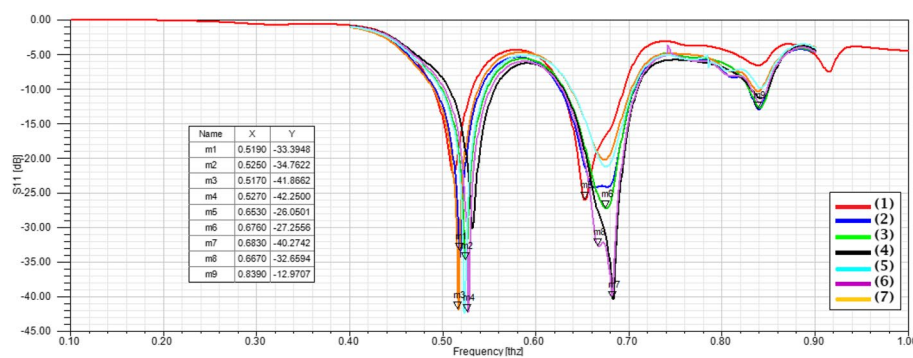
**Fig. 11** Simulated reflection coefficient (in dB)



**Fig. 12** Simulated antenna radiation pattern at 63.6 THz. **a** Conventional antenna. **b** Antenna-based DCB-SRR



**Fig. 13** Proposed shape of periodic arrays of the D-SRR in HFSS

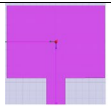
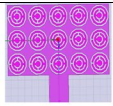
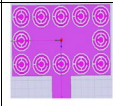
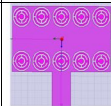
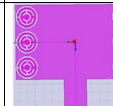
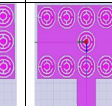
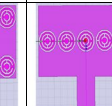


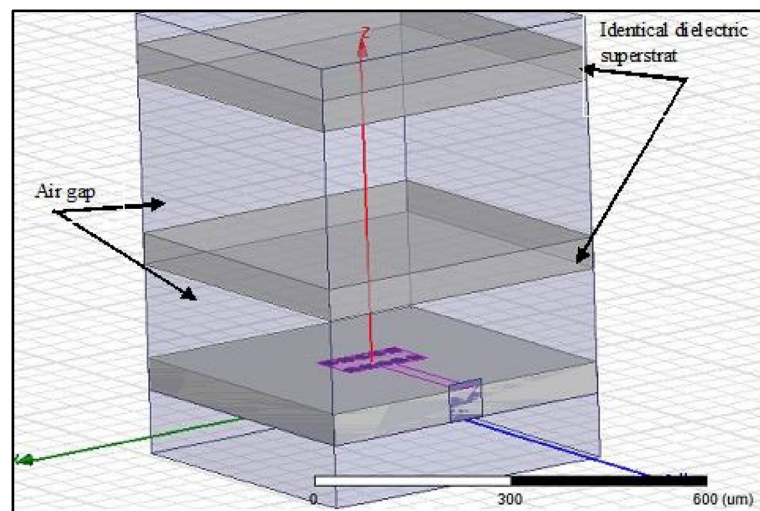
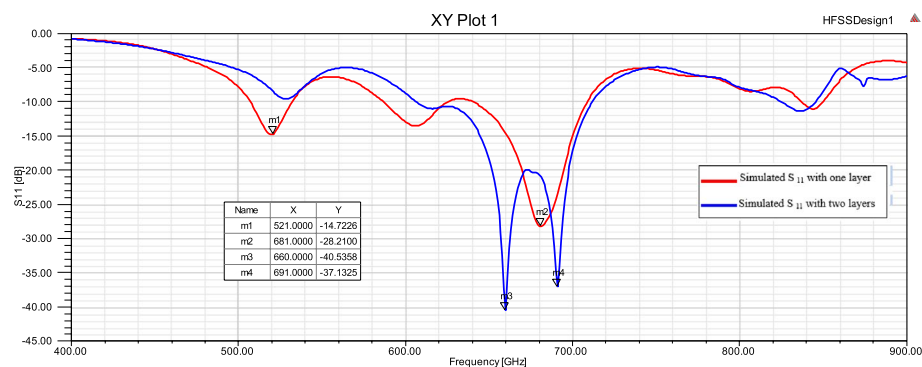
**Fig. 14** Simulated reflection coefficient of microstrip patch antenna loaded with periodic arrays D-SRR

displaces as the position of D-SRR is altered, in which the behavior analysis of the first mode enable to increase the bandwidth and the reflection coefficient in the antenna.

The electromagnetic wave is involved in view of the fact that the D-SRR reflects the wave back to the second ring and altering the ring's behavior, responsible for the permeability

**Table 3** Comparison of parameter results of microstrip patch antenna loaded with periodic arrays DSR

	(1)	(2)	(3)	(4)	(5)	(6)	(7)
Antenna							
$f_r$ (THz)	0.51-0.65	0.51-0.67	0.52-0.67	0.53-0.68	0.52-0.67	0.52-0.68	0.51-0.67
$S_{11}$ (dB)	-22.11 / -26.05	-34.36 / -24.06	-34.76 / -24.25	-30.10 / -40.19	-42.35 / -21.25	-42.25 / -32.77	-41.86 / -20.29
B(GHz)	40-30	50-80	50-70	50-80	50-70	50-80	40-70
G (dB)	5.04	3.81	3.89	3.78	3.74	3.81	3.75

**Fig. 15** Microstrip patch antenna with dielectric superstrate**Fig. 16** Reflection coefficients of microstrip patch antenna with dielectric superstrate

response and allowing to reduce mutual coupling while considering the rest of inner-ring rotation angles. However, it provides a decrease in a gain value to 5.04 dB from 3.89 dB compared to the conventional microstrip patch antenna.

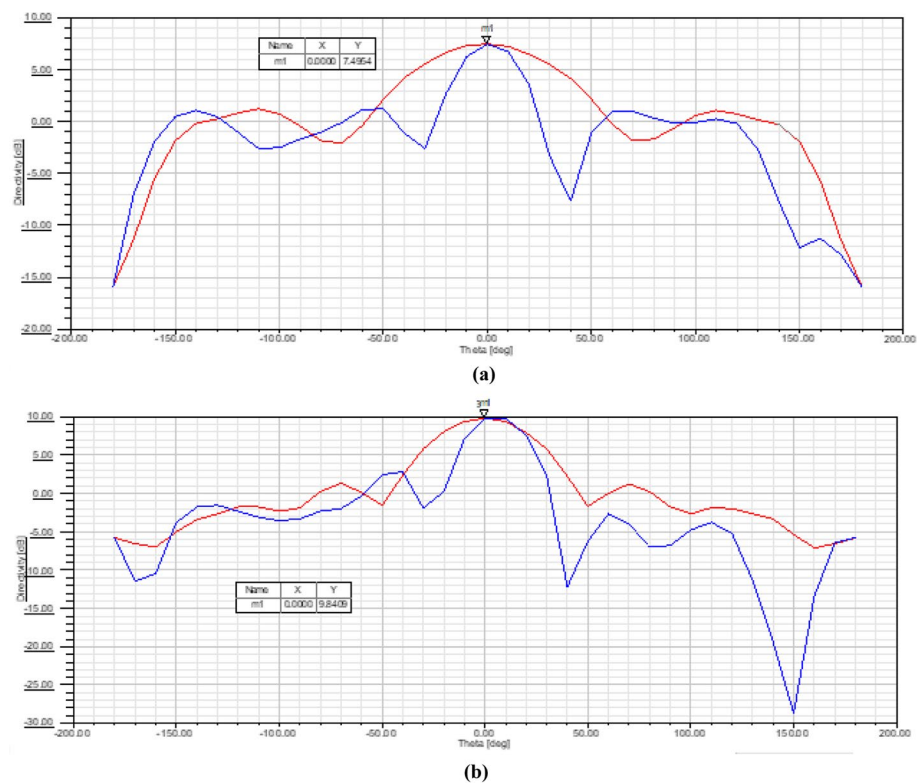


**Fig. 17** Directivity of microstrip patch antenna with dielectric superstrate. **a** Antenna with one layer. **b** Antenna with two layers

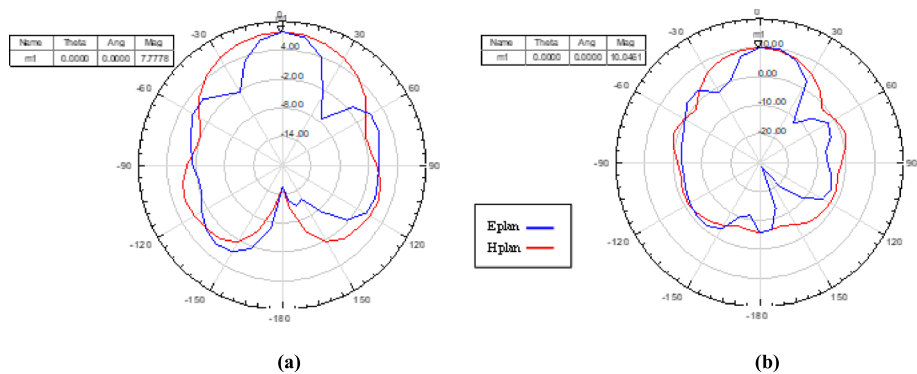


**Fig. 18** The radiation pattern of microstrip patch antenna with dielectric superstrate. **a** Antenna with one layer. **b** Antenna with two layers

*Microstrip patch antennas with dielectric superstrate* In order to further improve the gain and efficiency of the microstrip patch antenna and ensure the minimum impact on the antenna resonance frequency, we utilize the design of the periodic metamaterials D-SRR (4) established in the precedent section. The upper part of the antenna is covered with a “Rogers TMM 10 (tm)” ( $\epsilon_r = 9.2$ ) superstrate, consists of a one-dimensional electromagnetic band (1D-EBG) structure, made from two identical dielectric slabs [37].



**Table 4** Comparison study with existing works

References	Frequency band (THz)	Reflection coefficient (dB)	Bandwidth (GHz)	Directivity (dB)	Peak gain (dB)
[38]	0.5	−22	80	2.8	/
[39]	0.64–0.85	−35	/	5.6	/
[32]	0.69–0.77	−41.65/−25.30	224.7	/	10.43
[40]	0.69	−34.9	/	7.01	6.68
[35]	0.63	−44.71	/	8.61	7.94
[34]	0.67	/	/	5	5.22
[41]	0.69	/	/	6.59	5.74
This work	0.66–0.69	−40.53/−37.13	108	9.84	10.4

The first layer is adjusted about one third of the operation wavelength ( $\lambda/3$ ) above the ground plane which causes to gain increase. The distance of the second layer from the first layer is about  $\lambda/4$  [37]. To retain the same frequency band [0.4–0.9] THz, we adjusted the thickness of each layer to 50 $\mu\text{m}$  (Fig. 15).

The variation of the gain, directivity as well as of  $S_{11}$  with frequency, is illustrate in Figs. 16, 17 and 18, respectively.

The including of a double layer superstrate rectangular patch antenna cause the increase of reflection coefficient and affects the shape of the radiation pattern in both planes E and H.

The corresponding performances are summarized in Table 4.

Table 4 displayed the designed microstrip patch antenna with dielectric superstrate overall performance in comparison with previous works. The dielectric superstrate method always proved useful for microstrip antennas and provides better performances in terms of directivity and gain. The electric field is getting more strengths in the cavity regions created by the two layers of superstrates; as a result, we achieved a suitable percentage bandwidth, very high directivity, and gain at the terahertz band.

## Conclusions

The suggested antenna with different positions of dodecagon resonator on the substrate or on the rectangular patch produces multi-band posture and being possible to apply on distinct and specific frequencies (resonating under  $-10$  dB) on the band between 0.1 and 1 THz, as well as the resonator gap variations. The multiband frequency operation in antenna based on DBC-SRR is manifested in two ways: vertical position demonstrates the ability of beam deflection and horizontal position to optimize  $S_{11}$  frequency bandwidth. Furthermore, in this work, we have proposed a composed array of metamaterial unitary cells disposed periodically on the rectangular patch. The radiating frequencies can be designed to other desired values by making changes in the arrangements of the resonators and in slot parameters. The inclusion of the two same superstrate layers protects the microstrip patch as well as enhances

the antenna radiation characteristics. The use of higher ( $\epsilon_r = 9.2$ ) dielectric constant materials as a superstrate layer increases significantly the antenna directivity and gain, but it also reduces the bandwidth of the proposed antenna. Compared with the references, the microstrip patch antenna discloses a good performance in gain and radiation efficiency, meeting the design exigency. This structure can be extensively used in terahertz imaging and communication because of its amazing electrical, mechanical, and optical properties.

#### Abbreviations

SRR	Split-ring resonator
HFSS	High-frequency structure simulator
DBC-SRR	Dodecagon broadside-coupled split ring resonator
D-SRR	Dodecagon split ring resonator

#### Acknowledgements

We would like to acknowledge the support and guidance from Professor Zoubir MAHDJOUR during this research work.

#### Authors' contributions

All authors contributed to the manuscript and have read and approved the final version. KB performed the literature review, ZM realized the simulation and analysis, AB and MB were responsible for writing the manuscript and revisions.

#### Funding

This study had no funding from any resource.

#### Availability of data and materials

The datasets generated during and/or analyzed during the current study are available from the corresponding author on reasonable request.

#### Declarations

##### Ethics approval and consent to participate

Not applicable

##### Consent for publication

Not applicable

##### Competing interests

The authors declare that they have no competing interests.

Received: 5 April 2022 Accepted: 8 July 2022

Published online: 17 August 2022

#### References

1. Bala R, Marwaha A (2015) Characterization of graphene for performance enhancement of patch antenna in THz region. *Optik*
2. Devapriya AT, Robinson S (2019) Investigation on metamaterial antenna for terahertz applications. *J Microw Optoelectron Electromagn Appl* 18(3)
3. Song H-J, Nagatsuma T (2011) Present and future of terahertz communications. *IEEE Trans Terahertz Sci Technol* 1(1)
4. Prince, Kalra P, Sidhu E (2017) Rectangular terahertz microstrip patch antenna design for riboflavin detection applications. In: *International Conference on Big Data Analytics and Computational Intelligence (ICBDAC)*
5. Jha KR, Singh G (2010) Dual-band rectangular microstrip patch antenna at terahertz frequency for surveillance system. *J Comput Electron* 9:31–41
6. Adel-Rahmen M, Haraz OM, Ashraf N, Fakharzia M, Khaled U, Elshafiey I, Alshebeili S, RazikSebak A (2017) Properties of silica-based aerogel substrates and application to C-band circular patch antenna. *J Electron Mater*
7. Guha D, Antar YM (2010) *Microstrip and printed antennas: new trends, techniques and applications*, 1st edn. Wiley, New York
8. Keshwala U, Rawat S, Ray K (2020) Inverted K-shaped antenna with partial ground for THz applications. *Optik* 219:165092
9. Berka M, Azzeddine HA, Bendaoudi A, Mahdjoub Z, Rouabhi AY (2021) Dual-band bandpass filter based on electromagnetic coupling of twin square metamaterial resonators (SRRs) and complementary resonator (CSRR) for wireless communications. *J Electron Mater* 50:4887–4895
10. Smith D, Padilla W, Wier D, Nemat-Nasse S, Schultz S (2000) Composite medium with simultaneously negative permeability and permittivity. *Phys Rev Lett* 84:4184–4187



11. Bendaoudi A, Mahdjoub Z (2017) Comparative study of patch antenna loaded with slot split-ring resonators on different substrate materials. *Photon Netw Commun*
12. Pendry JB, Holden AJ, Robbins DJ, Stewart WJ (1999) Magnetism from conductors and enhanced nonlinear phenomena. *IEEE Trans Microw Theory Tech* 47(11):2075–2084
13. Rajo-Iglesias E, Quevedo-Teruel O, Ng MouKehn M (2009) Multiband SRR loaded rectangular waveguide. *IEEE Trans Antennas Propag* 57(5):1571–1575
14. Quevedo-Teruel O, Rajo-Iglesias E, Ng MouKehn M (2009) Numerical and experimental studies of split ring resonators loaded on the side walls of rectangular waveguides. *Microw Antennas Propag* 3(8):1262–1270
15. Marqués R, Martel J, Mesa F, Medina F (2002) Left-handed media simulation and transmission of EM waves in sub-wavelength SRR loaded metallic waveguides. *Phys Rev Lett* 89(18):183 901/1–4
16. Hrabar S, Bartolic J, Sipus Z (2005) Waveguide miniaturization using uniaxial negative permeability metamaterial. *IEEE Trans Antennas Propag* 53(1):110–119
17. Pucci E, Rajo-Iglesias E (2012) Malcolm Ng MouKehn, and Oscar Quevedo-Teruel, Enhancing the efficiency of compact patch antennas composed of split-ring resonators by using lumped capacitors. *IEEE Antennas Wirel Propag Lett* 11:1362–1365
18. Marqués R, Mesa F, Martel J, Medina F (2003) Comparative analysis of edge- and broadside-coupled split ring resonators for metamaterial design—theory and experiments. *IEEE Trans Antennas Propag* 51(10)
19. Simon SK, Chakraborty SP, Sebastian A, Jose J, Andrews J, Joseph VP (2019) Broadside coupled split ring resonator as a sensitive tunable sensor for efficient detection of mechanical vibrations. *Sensing Imaging* 20:1–1
20. Islam MT, Ashraf FB, Alam T, Misran N, Mat KB (2018) A compact ultrawideband antenna based on hexagonal split-ring resonator for pH sensor application. *Sensors (Basel)* 18(9):2959
21. Al-badri KSL, Abdulkarim YI, Alkurt FÖ, Karaaslan M (2021) Simulated and experimental verification of the microwave dual-band metamaterial perfect absorber based on square patch with a 45° diagonal slot structure. *J Electromagn Waves Appl* 35:issu 11
22. Yadgar A, Lian-wen D, Jun-liang Y, Şule Ç, Muharrem K, Sheng-xiang H, Long-hui H, Heng L (2020) Tunable left-hand characteristics in multi-nested square-split-ring enabled metamaterials. *J Central South Univ Corpus ID* 27(4):1235–1246
23. Saha C, Siddiqui JY, Antar YMM (2007) Theoretical investigation of the square split ring resonator. *Proc URSI NA Radio Sci Meet*
24. Saha C, Siddiqui JY (2009) Estimation of the resonance frequency of conventional & rotational circular split ring resonators. *IEEE Applied Electromagnetics Conference (AEMC), Kolkata*
25. Singh A, Sharma SK (2014) Calculation of resonant frequency of hexagonal split ring resonator using ANN. In: *URET: International Journal of Research in Engineering and Technology, IEEE Xplore*
26. Bilotti F, Toscano A, Vegni L, Aydin K, Alici KB, Ozbay E (2007) Equivalent-circuit models for the design of metamaterials based on artificial magnetic inclusions. *IEEE transactions on microwave theory and techniques*, vol. 55
27. Bilotti F, Toscano A, Vegni L (2007) Design of spiral and multiple split-ring resonators for the realization of miniaturized metamaterial samples. *IEEE transactions on antennas and propagation*, vol. 55
28. Vidyalakshmi MR, Raghavan S (2009) A CAD model of triangular split ring resonator based on equivalent circuit approach. *IEEE Applied Electromagnetics Conference (AEMC), Kolkata*
29. Sharma V, Pattnaik SS, Garg T, Devi S (2011) A microstrip metamaterial split ring resonator. *Int J Phys Sci* 6(4):660–663
30. Bose S, Ramaraja M, Raghavana S, Kumara S (2012) Mathematical modeling, equivalent circuit analysis and genetic algorithm optimization of an N-sided regular polygon split ring resonator (NRPSRR). *2<sup>nd</sup> International Conference on Communication, computing & Security. Proc Technoly* 6:763–770
31. da Silva JL, Chavesfernandes HC, de Andrade H, D (2016) Study of microstrip antenna behavior with metamaterial substrate of SRR type combined with TW. *Int J Commun*
32. Younssi M, Jaoujal A, Yaccoub MD, El Moussaoui A, Aknin N (2013) Study of a microstrip antenna with and without superstrate for terahertz frequency. *Int J Innov Appl Stud* 2(4):369–371
33. Nejati A, Sadeghzadeh RA, Geran F (2014) Effect of photonic crystal and frequency selective surface implementation on gain enhancement in the microstrip patch antenna at terahertz frequency. *Phys B* 449:113–120
34. Dhillon AS, Mittal D, Sidhu E (2017) THz rectangular microstrip patch antenna employing polyimide substrate for video rate imaging and homeland defence applications. *Optik* 144:634–641
35. Kushwaha RK, Karuppanan P, Malviya LD (2018) Design and analysis of novel microstrip patch antenna on photonic crystal in THz. *Phys B* 545:107–112
36. Abdelkarim M, Naoui S, Lassadlatrach, Gharsallah A (2017) Radiation efficiency improvement of RFID patch antenna using metamaterials. In: *International Conference on Green Energy Conversion Systems (GECS), IEEE xplore*
37. Errifi H, Baghdad A, Badri A, Sahel A (2016) Enhanced patch antenna performance using two layers dielectric superstrate in probe-Edgelnset and aperture feeding methods. *Int J Signal Process Syst* 4(5)
38. Zhang B et al (2015) Investigation on reconfigurable THz bowtie antenna based on graphene. In: *2015 IEEE 4th Asia-Pacific Conference on Antennas and Propagation (APCAP)*
39. Naghdehforushha SA, Moradi G (2017) Design of plasmonic rectangular ribbon antenna based on graphene for terahertz band communication. *IET Microw Antennas Propag* 12(5):804–807
40. Ullah S, Ruan C, Haq TU, Zhang X (2019) High performance THz patch antenna using photonic band gap and defected ground structure. *J Electromagn Waves Appl* 33(15):1943–1954
41. Tripathi SK, Kumar A, Manag. (2017) High gain highly directive graphene based terahertz antenna for wireless communication. *J Commun Eng Syst* 6:16

## Publisher's Note

Springer Nature remains neutral with regard to jurisdictional claims in published maps and institutional affiliations.